TISSUE ENGINEERING: Part C
Volume 18, Number 7, 2012

DOI: 10.1089/ten.tec.2011.0525

In Situ Tissue Engineering Using Magnetically Guided Three-Dimensional Cell Patterning

Shawn P. Grogan, Ph.D.,[1,2] Chantal Pauli, M.D.,[1,2] Peter Chen, Ph.D.,[1] Jiang Du, Ph.D.,[3] Christine B. Chung, M.D.,[3] Seong Deok Kong, Ph.D.,[4] Clifford W. Colwell, Jr., M.D.,[1] Martin K. Lotz, M.D.,[1,2] Sungho Jin, Ph.D.,[4] and Darryl D. D'Lima, M.D., Ph.D.[1,2]

Manipulation of cell patterns in three dimensions in a manner that mimics natural tissue organization and function is critical for cell biological studies and likely essential for successfully regenerating tissues—especially cells with high physiological demands, such as those of the heart, liver, lungs, and articular cartilage.[1,2] In the present study, we report on the feasibility of arranging iron oxide-labeled cells in three-dimensional hydrogels using magnetic fields. By manipulating the strength, shape, and orientation of the magnetic field and using crosslinking gradients in hydrogels, multi-directional cell arrangements can be produced *in vitro* and even directly *in situ*. We show that these ferromagnetic particles are nontoxic between 0.1 and 10 mg/mL; certain species of particles can permit or even enhance tissue formation, and these particles can be tracked using magnetic resonance imaging. Taken together, this approach can be adapted for studying basic biological processes *in vitro*, for general tissue engineering approaches, and for producing organized repair tissues directly *in situ*.

Introduction

Fabrication of complex tissues, such as liver, cardiac muscle, skin, bladder, and articular cartilage, has advanced through an assortment of tissue engineering and rapid prototyping techniques.[3–5] These approaches aim to mimic the orderly arrangement of cells within the organ, which is thought to provide cells with specific cell-to-cell and cell-to-extracellular matrix (ECM) microenvironments to collectively endow proper organ function.[6,7] Means to arrange cells in specific three-dimensional (3D) arrangements and to create appropriate microenvironments would represent major advancement in this field, which has been the focus of researchers in the tissue engineering field. However, many tissue prefabrication techniques rely on specialized equipment, bioreactors, and microfluidic devices or involve complicated procedures such as stereolithography, 3D printing, and selective laser sintering.[5,8–11] While these techniques are useful for understanding mechanisms of tissue regeneration, transferring these techniques into clinical tissue repair is still rudimentary. Specifically in regard to articular cartilage, the zonal arrangement of cells with unique differentiation status and gene expression profiles remains an important unmet goal in tissue engineering.

An alternative means to arrange cells and ECM for tissue engineering applications could be achieved through novel applications of nano- and micro-particles, particularly particles possessing super paramagnetic or ferromagnetic properties. Ferromagnetic nano- or micro-particles (FMP) dispersed in liquid and subjected to a unidirectional magnetic field can be arranged into various 3D interparticle configurations.[12–14]

FMP are especially suited for noninvasive tracking and directing labeled cells *in vivo*[15,16] and have been utilized for tissue engineering approaches, including seeding labeled cells into scaffolds[17] and for "magnetic force-based cell manipulation" for the arrangement of cell patterns in sheets for the construction of 3D multilayered tissues.[18,19] This approach has been used to create sheet layers of cells in patterns consisting of various cell types or for forming ring and tubular-like structures in urinary and vascular tissue engineering applications.[20–24] Magnetic organoid patterning[23] is a sophisticated example of employment of FMP in tissue engineering. This technique involves labeling cells with RGD-conjugated magnetic particles to produce multicelluar spheroids, which are manipulated via magnetic fields into distinct patterns for tissue production. While this approach is promising, it may not be appropriate for all tissues where a

[1]Shiley Center for Orthopaedic Research and Education, Scripps Clinic, La Jolla, California.
[2]Department of Molecular and Experimental Medicine, The Scripps Research Institute, La Jolla, California.
[3]Department of Radiology, School of Medicine, University of California–San Diego, San Diego, California.
[4]Department of Mechanical and Aerospace Engineering, University of California–San Diego, La Jolla, California.

3D alignment at the level of single cells, rather than spheres, may be more desirable or representative of the organ being reproduced. Most recently, an alternative and simple approach of cell patterning that combines photosensitive hydrogels and magnetic force has been described.[21]

In this study, we utilized the properties of FMP together with live cells and hydrogels to form neotissues with specific cellular organizations. This method relies on the binding of nano- or micron-sized iron oxide particles to cells, which are mixed into alginate hydrogels and crosslinked in calcium chloride solution, while subjected to specifically orientated external magnetic fields. The arrangement of cells in an *ex vivo* osteochondral defect model demonstrates the possibility of arranging cells directly *in situ*.

Methods and Materials

Cartilage procurement and chondrocyte isolation

Human articular cartilage was obtained at autopsy from normal tissue donors (approved by Scripps institutional review board). Chondrocytes were isolated from full-thickness cartilage shavings via enzymatic digestion and cultured in monolayer for one passage in DMEM (Mediatech Inc) supplemented with 10% calf serum (Omega Scientific Inc.) and penicillin/streptomycin/gentamycin (Invitrogen) as previously detailed.[25]

Magnetically responsive iron oxide particles

Three iron oxide materials were examined: (i) NanoArc industrial maghemite (Fe_2O_3), 20–40 nm (NArc); (ii) magnetite (Fe_3O_4) 97%–325 mesh (~44 μm) (MagN97); (iii) magnetite (Fe_3O_4) 98% 20–30 nm (MagN98). All materials were obtained from Alfa Aesar. Each particle was weighed and washed in 5 mL absolute ethanol once, centrifuged for 5 min at 2000 rpm, washed with phosphate-buffered saline (PBS) three times (5 mL), and finally resuspended in PBS at a weight to volume of 100 mg/mL. This mixture was heat-sterilized. The particles in PBS settle with gravity; after dispersion by vortex, all three particles show no signs of clumping or aggregation in the absence of a magnetic field.

Scanning electron microscopy of iron oxide particles

The size and shape of each type of the iron oxide particles were examined using scanning electron microscopy (SEM). The particles were dispersed in ethanol and then a droplet was placed on a silicon substrate. The dried particles were examined by high resolution SEM (XL30; FEI Co.).

Arrangement of cells labeled with iron oxide particles in alginate

The organization of cells within many tissues, including cartilage, is not uniform. To purposely alter the regional cellular patterns within one alginate gel, two systems were used in this study: (i) using a calcium chloride crosslinking gradient was made with temporal changes to the position of the magnetic field (Fig. 1) or (ii) by an arrangement of three magnets to create a region with specific magnetic field geometry (Fig. 2). For both approaches, chondrocytes were seeded in monolayer culture at a density of 50×10^3 cells per cm^2 and cultured for 24 h. MagN97 (1 mg/mL) was added to the cells in DMEM and incubated for 2 h before washing cells with PBS to remove unbound particles. Accutase (Innovative Cell Technologies) was added to detach cells and bound particles. The cells were mixed in 2% alginate (NovaMatrix) at a density for 8×10^6 per mL. To alter cellular arrangements within the same gel using the gradient approach (Fig. 1), cells in a 2% alginate mixture were transferred to a cell culture insert (8 μm; BD Biosciences). The insert was placed into a well of a 24-well plate containing 1 mL of $CaCl_2$ solution. A magnet was placed below the plate to align particles and cells in a vertical orientation (Fig. 1b). After 2 min, the magnet was placed adjacent (90°) to the plate to align the particles and cells that were in noncrosslinked portion of alginate (Fig. 1c). $CaCl_2$ solution was carefully added into the insert to affect crosslinking in both directions for another 20 min. The alignment of cells and particles was observed via light microscopy (Fig. 1d).

To determine a specific arrangement of magnets to provide a given magnetic field shape, commercially available software was used (Vizimag® release 3.193, Vizimag.com). A theoretical magnetic field shape using three magnets provided a region that simulated the type of cell arrangement that somewhat emulated articular cartilage cell arrangement of deep zone columns and tangential superficial zone cell alignment (Fig. 2a, b). A custom-made device was used to house three magnets in the predetermined configuration, with central well to place labeled cells in 2% alginate for alignment before crosslinking (Fig. 2c).

Magnets

Barium ferrite magnets (1×4×6 inch; 900 gauss) were used to arrange particles and cells in alginate, N45, and Ni-CU-Ni–coated rare earth neodymium disc magnet (10 lbs pulling force; 100–500 gauss).

Fusion of precrosslinked alginate gels

To fuse separate and already crosslinked alginate gels, we adopted a method previously described.[26] At least two different alginate gels-sheet/slabs were produced, as detailed above, using a polysulfone casting frame, containing MagN97 particles (1 mg/mL) were crosslinked with the particles aligned in a particular orientation. One gel comprised cells that were prelabeled with carboxyfluorescein succinimidyl ester (CSFE; Invitrogen) dye before MagN97 attachment to visualize cells after gel fusion and the other was unstained. Rectangular pieces of each gel-slab (~1×2 cm) were cut from each gel. Whatman filter paper, presoaked in a calcium-chelating solution of 82 mM sodium citrate (Sigma) in 4 mg/mL of noncrosslinked alginate, was placed on the upper surface of the CSFE-labeled gel for 2 min at room temperature. After removal of the filter paper, the unlabeled alginate gel with different MagN97 particle/cell alignment was immediately placed on top of the treated alginate for 8 min before treatment with a $CaCl_2$ solution described by Lee *et al*.[26] (80 mM $CaCl_2$, 49 mM NaCl, and 25 mM HEPES). Samples were maintained in the $CaCl_2$ solution for 15 min to crosslink alginate at the partially dissolved interface

Cell viability

MTT assay was used to determine potential toxicity of each iron oxide particle. Briefly, human chondrocytes were

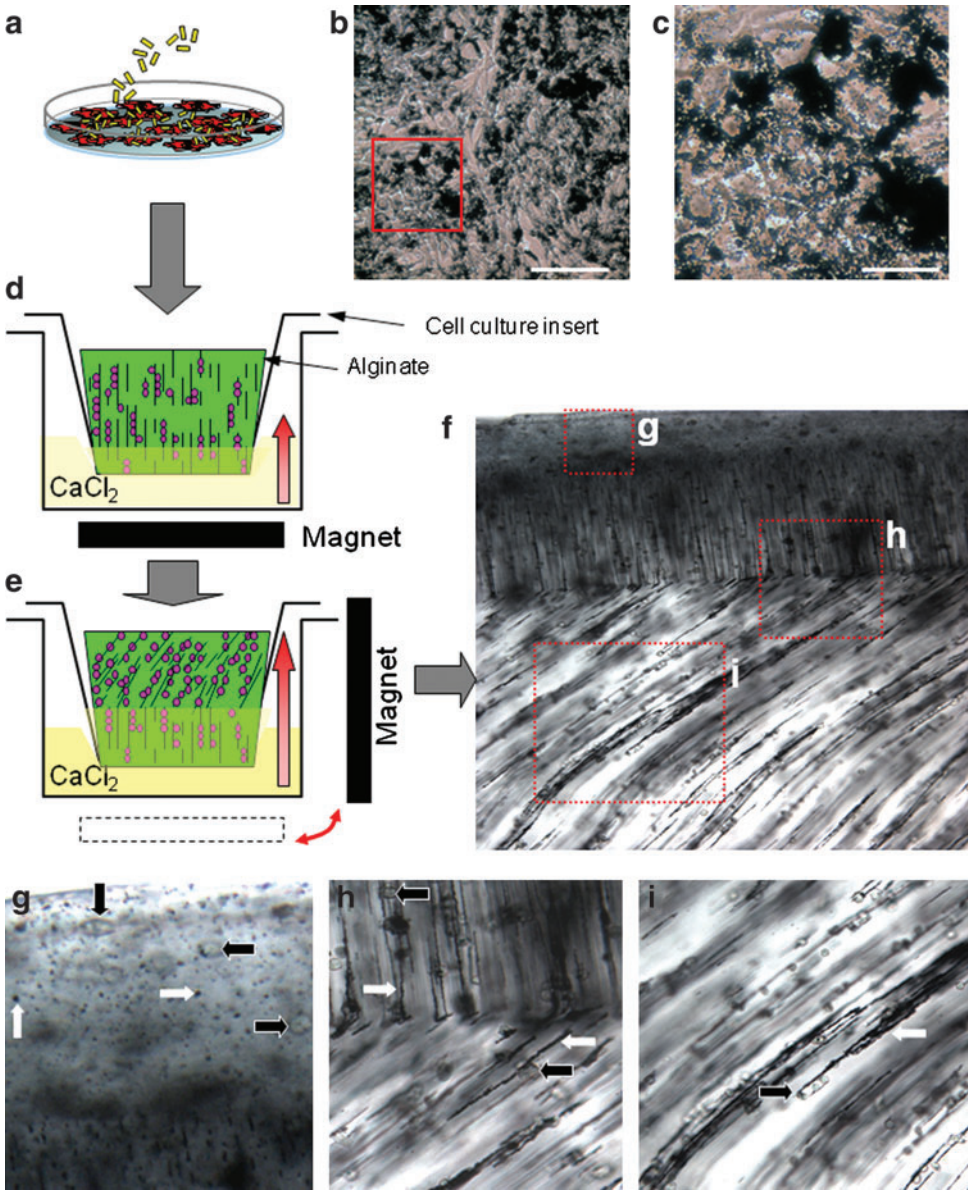

FIG. 1. Production of multiple cell arrangements in a single alginate gel using ferromagnetic particles and magnetic fields. **(a)** Human chondrocytes labeled with iron oxide particles (MagN97, 1 mg/mL) in culture. **(b)** Particles rapidly adhere to cells and **(c)** in 24 h, particles are either engulfed by the cell or remain associated with the cell surface. **(d)** Cells are harvested and mixed in 2% alginate, and transferred to a cell culture insert that is placed into a calcium chloride bath. The cells/particles are aligned vertically using an external magnetic field. The direction of alginate crosslinking is denoted by the bold red arrow. **(e)** After 2 min, the magnet was moved 90° to alter the alignment of the cells and bound particles. **(f)** The crosslinked alginate gel was cut via scalpel and visualized via light microscopy (40×) showing three regional arrangements. **(g)** Cells (bold black arrows) and particles (bold white arrows) on the surface are not organized. **(h)** Region showing transition between vertical alignment and diagonal arrangement. **(i)** Showing alignment of cells as a consequence of interaction with the magnetically aligned particles. Color images available online at www.liebertonline.com/tec

seeded in 96-well plates (5000 cells per well) and precultured overnight in DMEM with 2% calf serum. After preculture, the cells were exposed to 0.01, 0.1, and 1 mg/mL of each particle for 72 h. Assessment of cell viability was conducted via microplate reader at 540 nm. For longer-term assessments, human chondrocytes (8×10^6 cells per mL) were embedded in alginate with 0.1, 0.5, 1, 5, and 10 mg/mL of each particle and cultured in chondrogenic medium for 2 weeks. Live/dead staining (calcein-AM and ethidium homodimer-1) was performed as reported previously,[27] using confocal microscopy (LSM 510; Zeiss). The number of live cells was assessed using an image analysis script written in MATLAB (MathWorks). Viability is reported as percentage of live cells.

Pellet cultures

A number of human chondrocyte pellet cultures (5×10^5 each) were formed in the presence of NArc, MagN97, or MagN98 alone (1 mg/mL). All three materials were tested separately. Each pellet was cultured in serum-free ITS+ medium supplemented with TGFβ1 (10 ng/mL) as previously described[28] for 12 days and the medium was changed every 3 days. After 12 days, some pellets were fixed and embedded in paraffin for histology, while other pellets were prepared for RNA extraction for gene expression analysis.

RNA extraction and real-time polymerase chain reaction

Total RNA was isolated, from either the cultured cell pellets or the isolated cells cultured in 2% alginate, using the RNAeasy mini kit (Qiagen). First-strand cDNA synthesis was performed using total RNA as a template according to the manufacturer's protocols (Applied Biosystems). Quantitative real-time polymerase chain reaction was performed using TaqMan® gene expression reagents. *GAPDH* and *Col10a1*, *Col2a1*, *Col1a1*, and *aggrecan* (*AGG*) were detected using Assays-on-Demand™ primer/probe sets (Applied

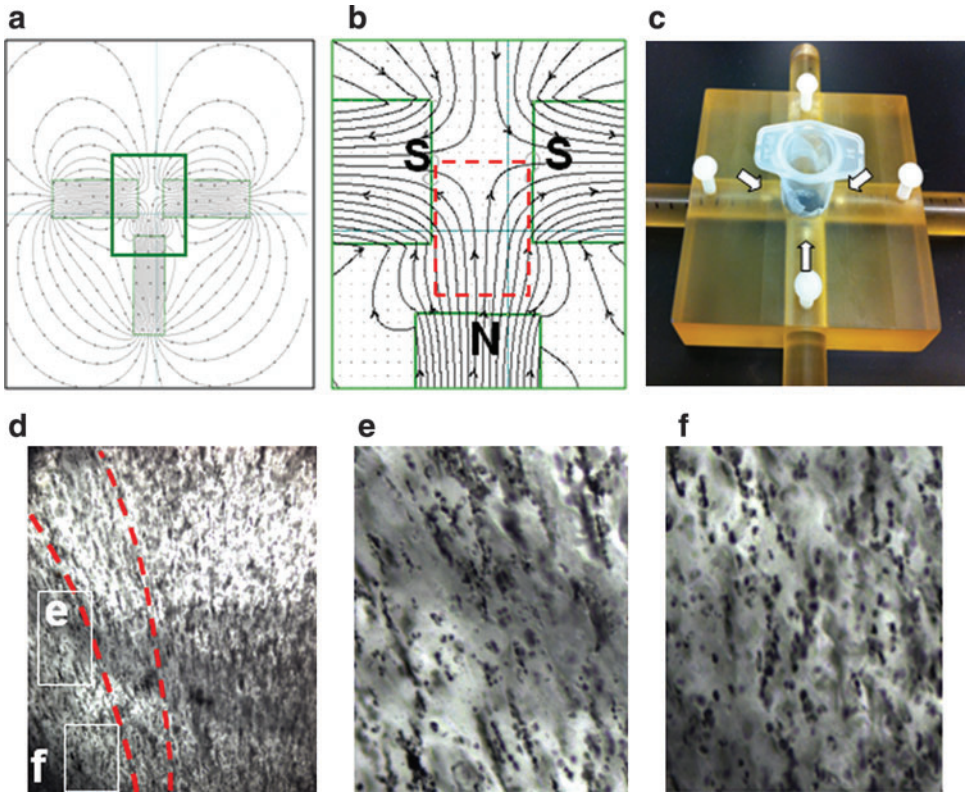

FIG. 2. Mapping magnetic field lines and application to produce curved cellular arrangements. **(a)** Theoretical magnetic field shape using three magnets (Vizimag .com). **(b)** Inset of theoretical magnetic field shape. **(c)** Device to hold three magnet configuration (white arrows indicate magnets) with a central well with cells in alginate. **(d)** Production of curved-labeled cells with the three magnet setup using MagN97 (1 mg/mL). **(e)** Showing inset of **(d)** with diagonal arrangement and **(f)** with vertical cell and particle arrangements in the same gel. Magnification for **(d)** is 10 ×. Color images available online at www.liebertonline.com/tec

Biosystems). Expression levels were normalized to *GAPDH* using the recommended ΔCt method, and fold-change was calculated using the $2^{-\Delta\Delta CT}$ formula.[29]

Histology and neocartilage grading (Bern Score)

Pellets of 12 days old were fixed in Z-Fix (ANATECH) and paraffin embedded. Sections of 4–5 μm were made for Safranin O-fast green staining. Immunohistochemical analyses of collagen type II were performed using conditions previously described.[30] Neocartilage quality was assessed (two observers) using the Bern Score,[31] which assesses the intensity of Safranin O stain, distance between cells, or the amount of ECM produced and cell morphology.

CSFE staining

Human chondrocytes cultured in T75cm^2 flasks were expanded to 70%–80% confluence in DMEM with 10% calf serum. A stock solution of 5 mM CFSE was diluted in 10 mL PBS to a final concentration of 5 μM and prewarmed to 37°C. Before applying the CSFE, the medium was removed and the cells were washed with PBS once before addition of the prewarmed CSFE/PBS solution. The cells were incubated for 15 min at 37°C. The CSFE solution was removed via aspiration and washed twice with PBS before adding fresh medium to the cells.

Arrangement of iron oxide particles in agarose

Each particle was suspended at 5 mg/mL in 1% agarose (UltraPure; Invitrogen) in the presence or absence of a magnetic field (~100 gauss). A dome of molten agarose-containing particles was allowed to gel at room temperature and sections were made to examine particle arrangements via phase-contrast light microscopy.

Multiple arrangements of iron oxide particles in the same alginate gel

MagN97 at 1 mg/mL was mixed in 2% alginate pipetted into a polysulfone casting frame 1 cm × 4 cm × 2.4 mm thick sandwiched between Whatman 3 mm filter paper held in place by stainless steel mesh and clamps and subsequently placed into a beaker containing a calcium chloride solution (120 mM $CaCl_2$, 150 mM NaCl, and 25 mM HEPES; Sigma). A barium ferrite magnet (1 × 4 × 6 inches), producing a magnetic field of ~100 gauss at the distance of samples, was placed below the crosslinking gel for 5 min and subsequently moved 90° to moved iron oxide particles within the gel that was not crosslinked. In some gels, the magnet was moved multiple times over a total time of 45 min while the entire gel slab was crosslinked. Sections of alginate were cut via scalpel and MagN97 arrangements were examined via light microscopy.

Mechanical property assessments

The mechanical property (stiffness) assessments of alginate gels with particles (aligned or nonaligned) at 1, 5, and 10 mg/mL and without particles were conducted using a custom-built device consisting of 2 miniature brushless servo actuators (SMAC), one 50 g load cell (FUTEK) with steel plunger having a flat surface for compression and LabVIEW (National Instruments) software for movement control and data acquisition on a laptop. The gels were placed between two 100-μm-thick cover slips and were loaded into the test chamber. The gel height was measured using the internal

linear encoder of the SMAC (1 μM resolution). A 5% of original height step compression was applied to the gel subsequently and the force was monitored and recorded. The gel was allowed to equilibrate for 2 min and then another 5% step compression was applied. The step compression was applied a total of 4 times, resulting in a net compression of 20%. Using the equilibrium force at each 5% compression level, Young's modulus was calculated.[32] Comparisons between control and MagN97 mixed gels were made using a *t*-test.

Cartilage explant defects

Osteochondral cores (6 mm) from porcine knees were harvested (OATS® system; Arthrex) and cultured in DMEM supplemented with 10% calf serum. Subchondral defects (3 mm wide and 2–3 mm deep) were produced in the center of each core using a 3-mm dermal punch (to define defect size) and a scalpel to remove the cartilage. MagN97-labeled chondrocytes or unlabeled cells (control) were mixed in 2% at a density of 8×10^6 cells per mL. Before crosslinking the alginate in $CaCl_2$ for 10 min, some defects were subject to a magnetic field of varying strengths (100–500 gauss) to align the cells in vertical columns within the defect. The explants were cultured for 1 week before being fixed (Z-fix) for 24 h and placed into 70% ethanol. These plugs were imaged using magnetic resonance imaging (MRI) and then decalcified for histological assessment.

Rabbit osteochondral defect model

Two osteochondral defects of 3.2 mm (wide) and 2 mm (deep) were formed in the trochlear groove of each knee of two 15-week-old New Zealand White (NZW) rabbits. (TSRI, IACUC Protocol Number: 09-0132). Monolayer-cultured NZW rabbit chondrocytes were either labeled with 5 mg/mL MagN97 or maintained unlabeled were suspended in 2% alginate and aseptically transferred into preassigned defects. Some defects were filled with control unlabeled cells (Ctrl); others were filled with MagN97-labeled cells. The alginate was crosslinked with $CaCl_2$. The rabbits were maintained for 4 weeks before euthanasia. Each rabbit knee was processed for MRI imaging and macroscopic evaluation.

Magnetic resonance imaging

The fixed osteochondral plugs containing labeled and unlabeled chondrocytes were imaged using 3D ultrashort TE (UTE) imaging using a 3T Signa TwinSpeed scanner (GE Healthcare Technologies) with a maximum gradient performance of 40 mT/m and 150 mT/m/ms. The 3D UTE sequence employed a short hard pulse (40 μs in duration) for nonselective excitation, followed by 3D radial ramp sampling with a minimum TE of 8 μs. Other imaging parameters included the following: TR = 31 ms, bandwidth = ±31.25 kHz, FOV = 4 cm, readout = 384, number of projections = 60,000, NEX = 1, flip angle = 9°, acquired voxel size = $104 \times 104 \times 104\ \mu m^3$, and scan time = 31 min.

Results

Multiple arrangements of cells in alginate labeled with iron oxide particles

We explored whether human chondrocytes labeled with iron oxide can be arranged in specific spatial patterns using external magnetic fields, which may facilitate regeneration of hyaline cartilage with its zonal architecture. Many hydrogels are biocompatible and permit neocartilage formation,[33] and while in the liquid phase, the labeled cells can be arranged into particular organizations and crosslinked to maintain permanent 3D patterns. We arranged iron-labeled chondrocytes into distinct patterns in alginate hydrogels before crosslinking in calcium chloride. Human chondrocytes were incubated with either MagN97 or NArc (1 mg/mL) for 24 h. These particles rapidly adhered to cells within 30–40 min and some particles were engulfed by the cells over 24 h. After removal of excess particles by washing in PBS, the cells were then detached, mixed into 2% alginate, and transferred into cell-culture inserts (Fig. 1). We positioned a magnet below the cell-culture insert for 2 min in the $CaCl_2$ solution to align the particle associated cells into vertical columns. After 2 min, the magnet was repositioned to 90° (perpendicular to the original orientation) for the remaining gelling time (20–30 min) to produce multi-cell/particle arrangements (Fig. 1f). Manipulation of cells in the manner using NArc (1 mg/mL) was also possible (Supplementary Fig. S1; Supplementary Data are available online at www.liebertonline.com/tec). We also demonstrated the ability to form various other particle-only organizations with alginate and agarose hydrogels (Supplementary Fig. S2). MagN97 iron oxide-labeled cells that were placed in the central chamber of the three-magnet system (Fig. 2c) organized cells in a manner that emulated the predicted curved pattern (Fig. 2d).

Fusion of alginate gels with different magnetic particle organizations

An alternative means to create spatially varying patterns of cells throughout a given engineering tissue is by fusing layers of precrosslinked alginate gels.[26] In this study, we formed two separate gels with differently organized iron oxide-labeled cells, either labeled or unlabeled with CSFE (green fluorescence), and then fused these gels together. Microscopic examination of these fused hydrogels show the interface regions and the distinct CSFE-positive and CSFE-negative portions, as well as particle orientations in each part of the fused construct (Fig. 3). This option opens the way to combine unique cell/particle arrangements to form multiphasic constructs that more accurately mimic tissues with differences in regional/zonal arrangements.

Normal cell viability and neo-cartilage formation in the presence of iron oxide particles

Iron oxide is well tolerated by mammalian cells.[34] Our viability/toxicity assessments of three different iron oxide particles confirm this observation with chondrocytes. One maghemite particle (Fe_2O_3, 20–40 nm; NArc) and two magnetite (Fe_3O_4) particles, MagN97 (~44 μm) and MagN98 (20–30 nm), showed no adverse effect on chondrocyte viability (~80% live cells) when mixed and cultured in alginate over several weeks (0.1 to 10 mg/mL). No release of toxins or change in cell viability was detected using iron oxide particles stored in PBS at room temperature for >12 months (Fig. 4a, b, and Supplementary Fig. S3).

To evaluate whether iron oxide particles are compatible with normal tissue formation, we analyzed human chondrocyte pellet cultures that accumulate cartilage ECM. Two

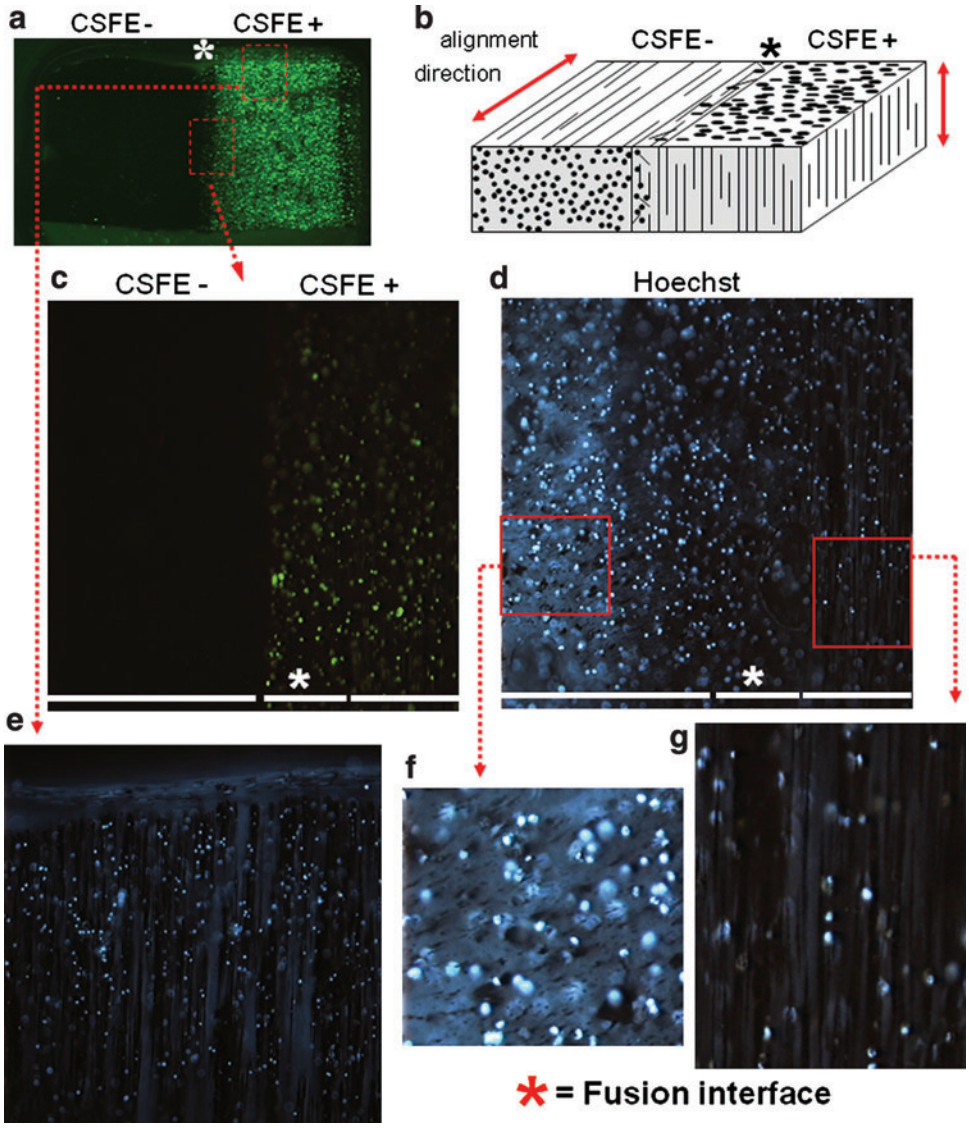

FIG. 3. Fusion of two alginate gels with different magnetic particle organizations. **(a)** Nonstained and carboxyfluorescein succinimidyl ester (CSFE)-stained (green) MagN97-labeled chondrocytes were separately mixed in 2% alginate, aligned using a magnetic field, and crosslinked (MagN97, 1 mg/mL). To fuse both gels, the surface of the CSFE gel was exposed to filter paper soaked with sodium citrate to partly dissolve the alginate gel surface for 2 min. The non-CSFE gel was placed on this interface for a further 8 min before the gels were fused by exposing the layered gels with $CaCl_2$. Cells from one gel were labeled with CSFE (Invitrogen) to better demark the interface region between the gels. Hoechst 33342 was used to visualize cells in both gels. **(b)** Cartoon indicating orientation of cell and MagN97 alignment and the interface region of the fused gels as denoted by an asterisk (*). **(c)** Higher magnification of selected region showing CSFE-positive and CSFE-negative regions and the interface area. **(d)** Hoechst 33342 staining showing the locality of cells in both gels. **(f, g)** Showing higher magnification of selected region showing cells and particle arrangements. **(e)** Hoechst 33342 staining image of the gel containing CSFE-labeled cells showing columnar arrangements of MagN97 particles and cells. Color images available online at www.liebertonline.com/tec

particles tested (NArc and MagN97) enhanced mRNA levels of two major cartilage-associated ECM genes (*Col2a1* and *aggrecan*) during tissue formation compared to control pellets (Fig. 4c) and displayed comparable levels of glycosaminoglycans (Fig. 4d) and collagen type II (Fig. 4e). MagN97 particles reduced *Col1a1* mRNA levels twofold and increase *Col10a1* levels twofold compared to controls (Fig. 4c). MagN98 particles did not promote the formation of neocartilage (Fig. 4c, d).

An added feature of neotissues formed using the iron oxide particles is the possibility of moving tissues using an external magnet. This process may be useful for less invasively moving delicate or nascent tissues in culture, to a precise target location or as a means to mechanically stimulate tissue. High-density cultures in a cell-culture insert system produced discs of neocartilage tissue that could be moved or levitated by an external magnet (Supplementary Fig. S4 and Supplementary Movie S1). High-density cultures produced with MagN97 and NArc resulted in neotissues with positive Safranin O stain (Supplementary Fig. S4a) and comparable mRNA levels of *aggrecan* and *Col2a1* as control (Supplementary Fig. S4b). MagN98 extensively reduced *Col2a1* and *aggrecan* gene

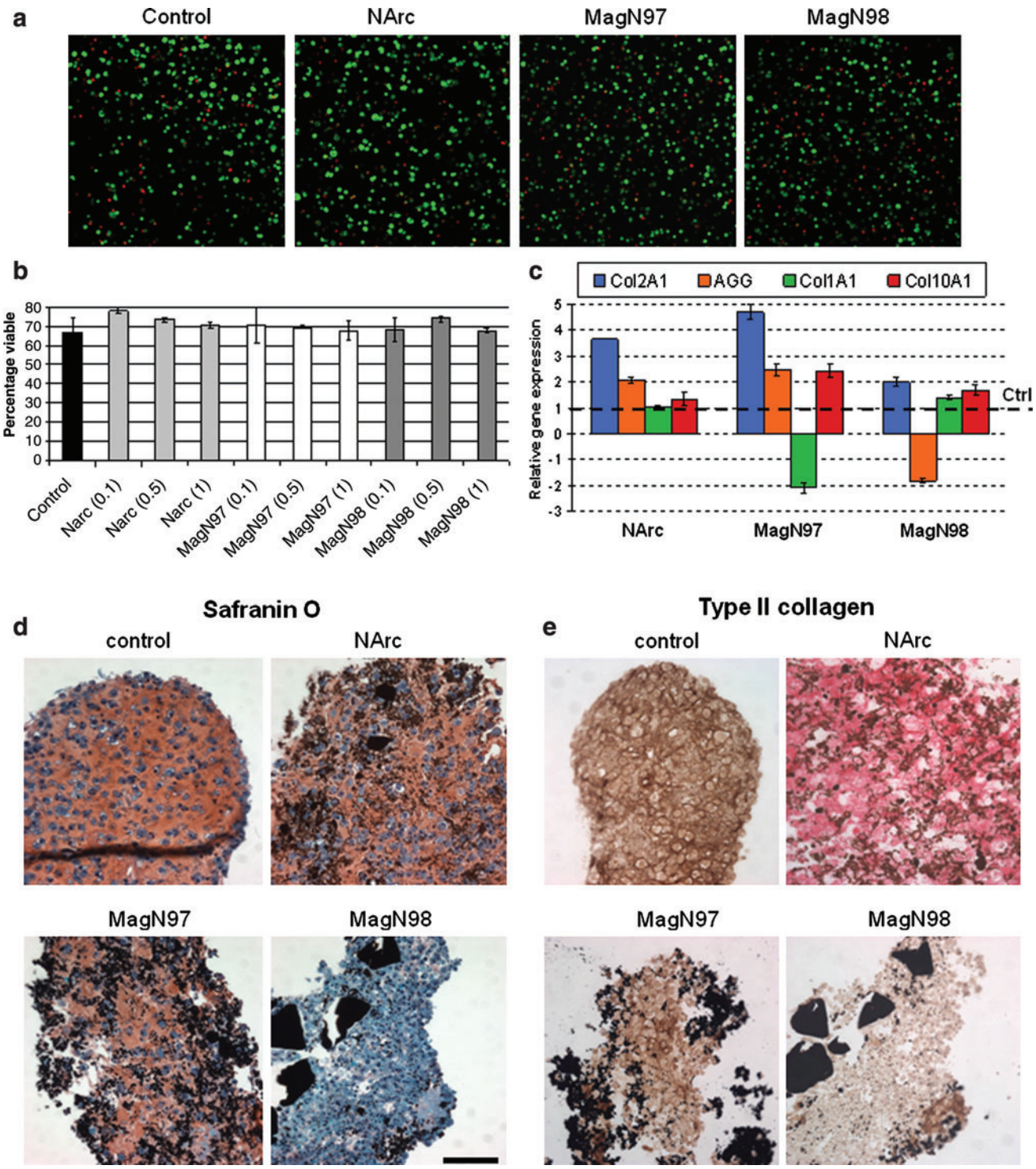

FIG. 4. Chondrocyte viability and neocartilage formation after exposure to iron oxide particles. **(a)** Confocal calcein AM (live, green) and ethidium homodimer-1 (dead, red) images of alginate cultures cultured with 1 mg/mL of NArc, MagN97, or MagN98 iron oxide particle for 14 days. **(b)** Percentage chondrocyte viability calculated from confocal images of alginate cultures subjected to 0.1, 0.5, and 1 mg/mL of each iron oxide particle. **(c)** Relative fold change in gene expression levels (*Col2a1*, *aggrecan* [*AGG*], *Col1a1*, and *Col10a1* relative to control [Ctrl]) in 12-day cultivated pellet cultures in the presence of 1 mg/mL of each iron oxide particle. **(d)** Safranin O staining of pellets cultivated for 12 days to visualize glycosaminoglycan deposition (Bern scores: control = 7.8 ± 0.3, NArc = 7.3 ± 0.3, MagN97 = 6.5 ± 0.5), and MagN98 scores indicated poor tissue quality (3.5 ± 0.5) and **(e)** type II collagen deposition (scale bar, 50 μm). Color images available online at www.liebertonline.com/tec

expression similar to the pellet cultures (Fig. 4c). MagN97 induced less *Col10a1* gene expression than MagN98: two- versus sevenfold increase compared to controls, respectively, in the high-density culture system.

Mechanical properties of hydrogels altered by particle orientation

We examined whether the addition of MagN97 into 2% hydrogels may change mechanical properties. We hypothesized that the gel stiffness would be altered by particle orientation within the gel. Young's modulus was only significantly increased in gels containing vertically aligned MagN97 at 10 mg/mL (Supplementary Table S1; $p < 0.02$). Conversely, randomly mixed or nonaligned MagN97 particles at 10 mg/mL were significantly less stiff ($p < 0.04$). The decrease in stiffness in the random gels is likely due to interference in the crosslinking process with increased particles throughout the gel. In the aligned gels, it speculated that both the formation of columns and the creation of particle-free areas allowing normal crosslinking (see examples in Fig.3e, g) contribute to increased gel stiffness. Controlling the concentration and orientation of the particles within the gels provides an additional means of modulating mechanical properties of engineered tissues, particularly in demanding *in vivo* environments.

Optimization of particle concentration and field strengths of labeled cells in a bovine osteochondral defect model

The ease of labeling cells and the ability for remote manipulation conceptually provides an opportunity to implant and organize cells directly into the target tissues. We surgically created cartilage defects in bovine osteochondral explants. Labeled cells were suspended in alginate, applied to the defects, organized with a magnetic field, and cultured for 2 weeks (Fig. 5a). Defects filled with MagN97-labeled chondrocytes (Fig. 5b) demonstrated loss of MRI signal indicative of the presence of iron oxide compared to defects filled with unlabeled cells. After 2 weeks of culture, repair tissue formed by iron-labeled and arranged cells appeared to be of higher quality compared to control nonlabeled cells (Supplementary Fig. S5). Optimal cell MagN97 labeling and magnetic field settings indicated that between 1 and 10 mg of iron oxide added to 3×10^6 cells in monolayer culture (T175cm^2 flask) was sufficient to label cells and ~500 gauss was needed to reproducibly arrange cells in the defects (Fig. 5c, d).

Development of an in vivo *model*

For initial proof of concept *in vivo*, we employed a rabbit osteochondral defect model to test surgical implantation and retention (Fig. 5e–h) and to examine whether the cells can be tracked by MRI. Knees imaged through MRI after 4 weeks clearly identified defects that were either labeled or unlabeled with MagN97 (Fig. 5h). Macroscopic assessment showed that the implants remained in the defects and signs of early defect healing (Fig. 5i).

SEM results

The sizes of the particles determined by SEM (Supplementary Fig. S6) were generally consistent with the manufacture's description with the exception of MagN97, which was categorized as −325 mesh or ~44 μm. The SEM analysis indicated that MagN97 iron oxide particles are on average ~200 nm in diameter with wide variation from ~70 to ~500 nm range and with shapes ranging from spherical to elongated/oval. SEM determined that NArc particles to possess an average diameter of ~50 nm (distribution from ~10 to ~100 nm), with relatively tight and uniform particle size. For MagN98, particles were on average ~30 nm in diameter and ranged in size from 10 to 40 nm, displaying a relatively tight and uniform particle size. Some NArc and MagN98 particles are slightly faceted.

Discussion

Over the past decade many innovative approaches have been developed toward manipulating cells, either actively or passively, using complex and simple technologies. Fu *et al*.[21] provide an excellent overview of these approaches. The end goal of these efforts is for the creation of cell patterns in 3D that emulate organs for studies on how such organizations will effect cell–cell and/or cell–ECM interactions, but also for eventual use in a clinical setting as a cell-based therapy.

By combining the unique attributes of iron oxide particles, hydrogels, and magnetic fields, we have demonstrated the feasibility of manipulating cells into various patterns that mimic natural tissue. These particles are nontoxic and permit or even enhance neocartilage formation. The properties of iron oxide also permit the use of MRI to monitor labeled cells *in vivo*. The techniques shown here are also relatively simple to use and do not require sophisticated equipment. We show the possibility of forming cellular patterns in 3D alginate hydrogels with specific magnetic field shapes, or by fusing together layers of gels with prearranged cellular arrangements. For the latter approach, further testing for the shear strength of fused layers would be needed if such constructs are destined for *in vivo* implantation. However, the mechanical stability may be secondary for *in vitro* studies to examine the effect of co-culturing cells in different layers and with various cellular arrangements to better emulate a natural tissue or organ.

Although we utilized alginate hydrogels, it is plausible to use other materials such as agarose (see Supplementary Fig. S2), hyaluronan-based hydrogels,[35] or photo-crosslinkable PEG[36] for instance. Collectively, this approach holds promise for the creation of organized repair tissues directly *in situ*. The more complicated feature of our approach, at least *in situ*, would be the creation of complex magnetic field shapes, if indeed required, at the repair site.

In terms of meeting medical needs, osteoarthritis (OA) and other rheumatic diseases are among the most common of all health conditions and are the number one cause of disability in the United States, affecting an estimated 27 million Americans in 2008.[37] The economic impact of arthritis in the United States is estimated at $128 billion per year, representing >2% of the gross domestic product.[38] Only symptom-modifying therapies are used to treat OA.[39,40] For two decades, only one major cell-based tissue regeneration strategy, autologous cell implantation, is clinically employed. However, this procedure does not predictably result in functional hyaline cartilage, but rather in fibrocartilage,[41,42] which lacks the cellular and ECM organization required to support the demanding load-bearing functions of this

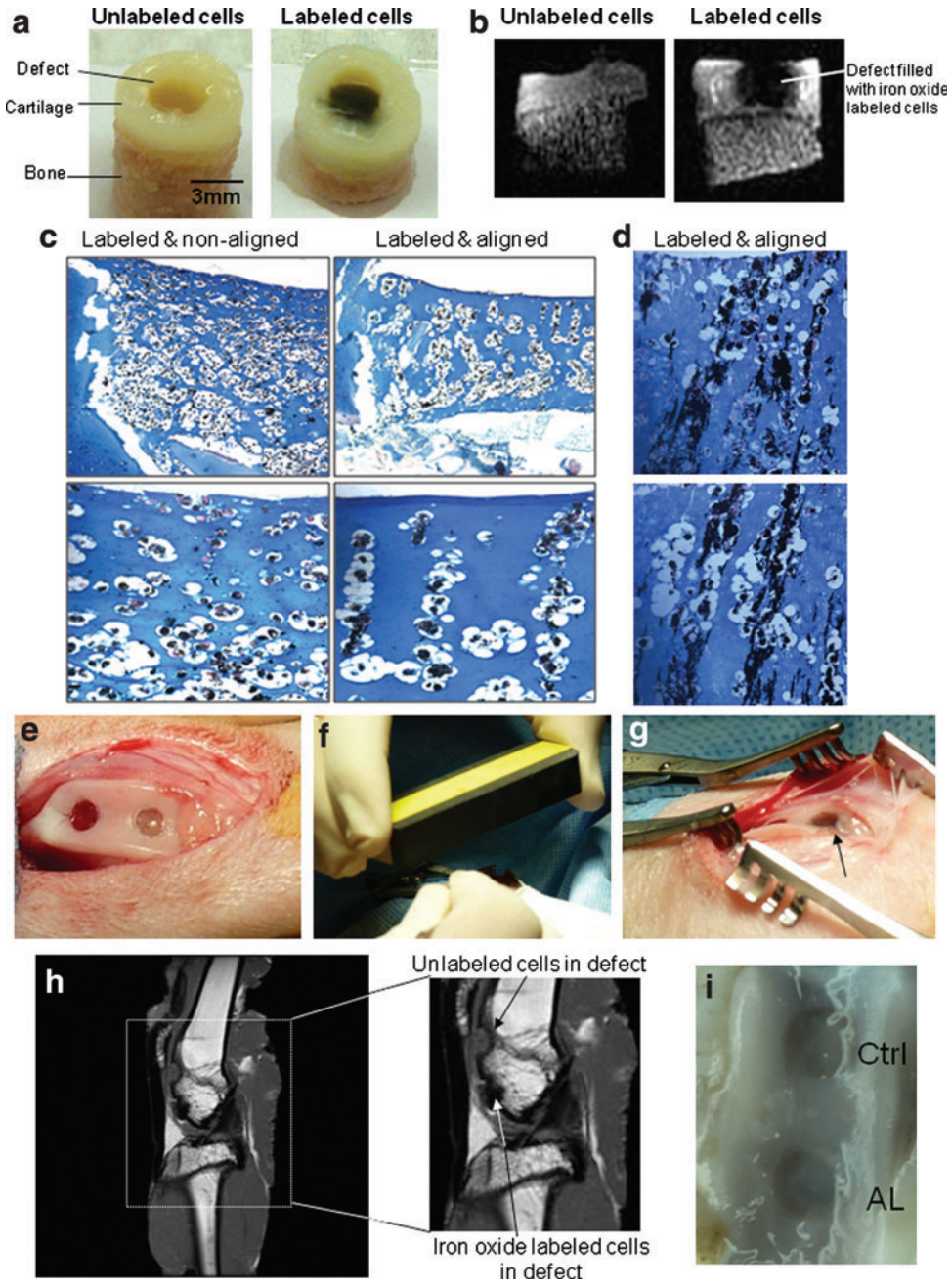

FIG. 5. Organization of cells guided by external magnetic fields in cartilage explants defect and in an *in vivo* cartilage repair model. **(a)** Bovine osteochondral cores (6 mm diameter) with a 3-mm central defect filled with either unlabeled cells or MagN97-labeled cells in alginate (20×10^6 cells per defect). Labeled cells were either aligned or nonaligned. **(b)** Magnetic resonance imaging (MRI) of defects filled with labeled or unlabeled chondrocytes using 3D ultrashort TE sequences. The presence of iron oxide-labeled cells is reflected in a loss of signal. **(c)** Optimized labeling (5 mg/mL, MagN97) and magnetic field settings (>500 gauss) to reproducibly form cell columns (magnification 4×, 10×, and 40×). **(d)** Chondrocyte and MagN97 (10 mg/mL) arrangement (magnification 40×). **(e)** Defects in trochlear groove (3.2×2 mm deep). **(f)** Alignment of iron oxide-labeled cells via external magnet (~500 gauss). **(g)** Defect filled with iron oxide-labeled cells in cross-linked alginate (arrow). **(h)** MRI images of rabbit knee showing defects implanted with either unlabeled or labeled cells. **(i)** Macroscopic image of defects after 4 weeks of cell implantation (Ctrl, control nonlabeled; AL, labeled and magnetically aligned treated defect). Color images available online at www.liebertonline.com/tec

tissue.[3,26] Although *in vitro* prefabrication of tissue grafts has shown variable success in animal models[43] and cartilage tissues engineered with zonal organization have improved to provide a natural spatial cell distribution,[3,44–47] these approaches have not been transferred to a clinical setting. The procedures outlined above are laborious and expensive. Our approach offers a means to circumvent these deficiencies to produce organized tissues *in situ* with specific cellular organizations that mimic the native tissue.

Labeling cells with iron oxide does not appear to effect chondrocyte or mesenchymal stem cell (MSC) function or differentiation potential,[48–50] although Kostura *et al.*[51] indicated a negative effect on MSC chondrogenesis. While the effect of these particles supports neocartilage formation, particle species and size are likely to be important factors affecting cell phenotype. MagN97 particles demonstrated better neocartilage potential by increasing expression of *Col2a1* and *aggrecan* and reducing *Col1a1* expression. The increased expression of *Col10a1* is of concern and merits further study. It is also possible that optimizing particle size may improve cell function since average particle size for MagN97 (~200 nm) was substantially larger than that for NArc (~50 nm) and MagN98 (~30 nm). The interaction of the cells with the particles needs further study, including what proportion of the iron oxide is phagacytosed by the cells and how this may affect cell function following magnetic field application. The long-term effect of harboring iron oxide particles in the body is unclear. Another feature of creating organized tissues *in situ* is whether such arrangements will be maintained in the body or will be extensively remodeled. From our observations, the organization

of cells in crosslinked alginate is stable over months in culture, but reaction to the hydrogel and/or particles may be compromised over time.

We hypothesize that the arrangement of cells and ECM proteins closer to the natural structure would represent a good template to support development of neo tissues and perhaps guide better tissue formation, maturity, and its longevity. A proposed future possibility, to further augment the use of these particles, would include coating the particles with specific proteins (e.g., specific growth factors and ECM proteins) to further stimulate tissue formation and promote the development specific cell phenotypes.

Acknowledgments

Funding was provided by California Institute of Regenerative Medicine (TR1-01216), National Institutes of Health (P01 AG007996), The Scripps Translational Science Institute (UL1 RR025774), Donald and Darlene Shiley, UC Discovery Grant (ele08-128656/Jin) and, partially funded by an AOSSM-Genzyme grant. We greatly appreciate technical assistance by Jianfen Chen (gene expression analyses), Nick Steklov and Xian Chen (mechanical testing), Juan Hermida (animal surgery), Lilo Creighton (histology), Greame Bydder (MRI), Michelle Cheung (magnetic field mapping), and Judy Blake (manuscript formatting and copyediting). Antibodies used in this study were obtained from the Developmental Studies Hybridoma Bank developed under the auspices of the National Institute for Child Health and Human Development (NICHD) and maintained by Department of Biology, The University of Iowa, Iowa City, IA 52242.

Authors' Contributions

S.P.G., S.J., and D.D.D. orchestrated overall experimental design. S.P.G. and D.D.D. wrote the article in close collaboration with the other authors. S.P.G. designed and conducted cell culture studies and analyses. C.P. designed and conducted histology and analysis. P.C. and S.J. contributed to generation of appropriate magnetic fields. S.D.K. and S.J. conducted and interpreted the SEM analysis. J.D. and C.B.C. orchestrated the MRI study design and image analysis. All authors discussed the results and approved the final version of the article.

Disclosure Statement

The authors declare no competing financial interests.

References

1. Akiyama, H., Ito, A., Kawabe, Y., and Kamihira, M. Fabrication of complex three-dimensional tissue architectures using a magnetic force-based cell patterning technique. Biomed Microdevices **11,** 713, 2009.
2. Griffith, L.G., and Swartz, M.A. Capturing complex 3D tissue physiology *in vitro*. Nat Rev Mol Cell Biol **7,** 211, 2006.
3. Klein, T.J., Malda, J., Sah, R.L., and Hutmacher, D.W. Tissue engineering of articular cartilage with biomimetic zones. Tissue Eng Part B Rev **15,** 143, 2009.
4. Vunjak-Novakovic, G., Tandon, N., Godier, A., Maidhof, R., Marsano, A., Martens, T.P., *et al.* Challenges in cardiac tissue engineering. Tissue Eng Part B Rev **16,** 169, 2010.
5. Wang, X., Yan, Y., and Zhang, R. Recent trends and challenges in complex organ manufacturing. Tissue Eng Part B Rev **16,** 189, 2010.
6. Du, Y., Lo, E., Ali, S., and Khademhosseini, A. Directed assembly of cell-laden microgels for fabrication of 3D tissue constructs. Proc Natl Acad Sci U S A **105,** 9522, 2008.
7. Rivron, N.C., Rouwkema, J., Truckenmuller, R., Karperien, M., De Boer J., and Van Blitterswijk, C.A. Tissue assembly and organization: developmental mechanisms in microfabricated tissues. Biomaterials **30,** 4851, 2009.
8. Andersson, H., and van den Berg, A. Microfabrication and microfluidics for tissue engineering: state of the art and future opportunities. Lab Chip **4,** 98, 2004.
9. Kaji, H., Camci-Unal, G., Langer, R., and Khademhosseini, A. Engineering systems for the generation of patterned cocultures for controlling cell-cell interactions. Biochim Biophys Acta **1810,** 239, 2011.
10. Khademhosseini, A., Langer, R., Borenstein, J., and Vacanti, J.P. Microscale technologies for tissue engineering and biology. Proc Natl Acad Sci U S A **103,** 2480, 2006.
11. Okuyama, T., Yamazoe, H., Mochizuki, N., Khademhosseini, A., Suzuki, H., and Fukuda, J. Preparation of arrays of cell spheroids and spheroid-monolayer cocultures within a microfluidic device. J Biosci Bioeng **110,** 572, 2010.
12. Jin, S., Sherwood, R.C., Mottine, J.J., Tiefel, T.H., Opila, R.L., and Fulton, J.A. New Z-direction anisotropically conductive composites. J Appl Phys **64,** 6008, 1988.
13. Jin, S., Tiefel, T.H., Wolfe, R., Sherwood, R.C., and Mottine, J.J., Jr. Optically transparent, electrically conductive composite medium. Science **255,** 446, 1992.
14. McCormack, M., Jin, S., and Kammlott, G. Enhanced solder alloy performance by magnetic dispersions. IEEE Trans CPMT **17,** 452, 1994.
15. Arbab, A.S., Jordan, E.K., Wilson, L.B., Yocum, G.T., Lewis, B.K., and Frank, J.A. *In vivo* trafficking and targeted delivery of magnetically labeled stem cells. Hum Gene Ther **15,** 351, 2004.
16. Henning, T.D., Boddington, S., and Daldrup-Link, H.E. Labeling hESCs and hMSCs with iron oxide nanoparticles for non-invasive *in vivo* tracking with MR imaging. J Vis Exp **(13),** pii: 685, 2008.
17. Shimizu, K., Ito, A., and Honda, H. Enhanced cell-seeding into 3D porous scaffolds by use of magnetite nanoparticles. J Biomed Mater Res B Appl Biomater **77,** 265, 2006.
18. Ito, A., Hayashida, M., Honda, H., Hata, K., Kagami, H., Ueda, M., *et al.* Construction and harvest of multilayered keratinocyte sheets using magnetite nanoparticles and magnetic force. Tissue Eng **10,** 873, 2004.
19. Ito, A., Takizawa, Y., Honda, H., Hata, K., Kagami, H., Ueda, M., *et al.* Tissue engineering using magnetite nanoparticles and magnetic force: heterotypic layers of cocultured hepatocytes and endothelial cells. Tissue Eng **10,** 833, 2004.
20. Frasca, G., Gazeau, F., and Wilhelm, C. Formation of a three-dimensional multicellular assembly using magnetic patterning. Langmuir **25,** 2348, 2009.
21. Fu, C.Y., Lin, C.Y., Chu, W.C., and Chang, H.Y. A simple cell patterning method using magnetic particle-containing photosensitive poly (ethylene glycol) hydrogel blocks: a technical note. Tissue Eng Part C Methods **17,** 871, 2011.
22. Ito, A., Akiyama, H., Kawabe, Y., and Kamihira, M. Magnetic force-based cell patterning using Arg-Gly-Asp (RGD) peptide-conjugated magnetite cationic liposomes. J Biosci Bioeng **104,** 288, 2007.
23. Lin, R.Z., Chu, W.C., Chiang, C.C., Lai, C.H., and Chang, H.Y. Magnetic reconstruction of three-dimensional tissues from multicellular spheroids. Tissue Eng Part C Methods **14,** 197, 2008.
24. Yamamoto, Y., Ito, A., Kato, M., Kawabe, Y., Shimizu, K., Fujita, H., *et al.* Preparation of artificial skeletal muscle

tissues by a magnetic force-based tissue engineering technique. J Biosci Bioeng **108,** 538, 2009.
25. Blanco, F.J., Ochs, R.L., Schwarz, H., and Lotz, M. Chondrocyte apoptosis induced by nitric oxide. Am J Pathol **146,** 75, 1995.
26. Lee, C.S., Gleghorn, J.P., Won Choi, N., Cabodi, M., Stroock, A.D., and Bonassar, L.J. Integration of layered chondrocyte-seeded alginate hydrogel scaffolds. Biomaterials **28,** 2987, 2007.
27. Grogan, S.P., Aklin, B., Frenz, M., Brunner, T., Schaffner, T., and Mainil-Varlet, P. *In vitro* model for the study of necrosis and apoptosis in native cartilage. J Pathol **198,** 5, 2002.
28. Barbero, A., Grogan, S., Schafer, D., Heberer, M., Mainil-Varlet, P., and Martin, I. Age related changes in human articular chondrocyte yield, proliferation and post-expansion chondrogenic capacity. Osteoarthritis Cartilage **12,** 476, 2004.
29. Livak, K.J., and Schmittgen, T.D. Analysis of relative gene expression data using real-time quantitative PCR and the 2 (-Delta Delta C(T)) Method. Methods **25,** 402, 2001.
30. Grogan, S.P., Miyaki, S., Asahara, H., D'Lima, D.D., and Lotz, M.K. Mesenchymal progenitor cell markers in human articular cartilage: normal distribution and changes in osteoarthritis. Arthritis Res Ther **11,** R85, 2009.
31. Grogan, S.P., Barbero, A., Winkelmann, V., Rieser, F., Fitzsimmons, J.S., O'Driscoll, S., *et al.* Visual histological grading system for the evaluation of *in vitro*-generated neocartilage. Tissue Eng **12,** 2141, 2006.
32. Korhonen, R.K., Laasanen, M.S., Toyras, J., Rieppo, J., Hirvonen, J., Helminen, H.J., *et al.* Comparison of the equilibrium response of articular cartilage in unconfined compression, confined compression and indentation. J Biomech **35,** 903, 2002.
33. Noth, U., Steinert, A.F., and Tuan, R.S. Technology insight: adult mesenchymal stem cells for osteoarthritis therapy. Nat Clin Pract Rheumatol **4,** 371, 2008.
34. Dobson, J., Bowtell, R., Garcia-Prieto, A., and Pankhurst, Q. Safety implications of high-field MRI: actuation of endogenous magnetic iron oxides in the human body. PLoS One **4,** e5431, 2009.
35. Jin, R., Moreira Teixeira, L.S., Krouwels, A., Dijkstra, P.J., van Blitterswijk, C.A., Karperien, M., *et al.* Synthesis and characterization of hyaluronic acid-poly(ethylene glycol) hydrogels via Michael addition: an injectable biomaterial for cartilage repair. Acta Biomater **6,** 1968, 2010.
36. Hou, Y., Schoener, C.A., Regan, K.R., Munoz-Pinto, D., Hahn, M.S., and Grunlan, M.A. Photo-cross-linked PDMSstar-PEG hydrogels: synthesis, characterization, and potential application for tissue engineering scaffolds. Biomacromolecules **11,** 648, 2010.
37. Lawrence, R.C., Felson, D.T., Helmick, C.G., Arnold, L.M., Choi, H., Deyo, R.A., *et al.* Estimates of the prevalence of arthritis and other rheumatic conditions in the United States. Part II. Arthritis Rheum **58,** 26, 2008.
38. Centers for Disease Control and Prevention (CDC). National and state medical expenditures and lost earnings attributable to arthritis and other rheumatic conditions—United States, 2003. MMWR Morb Mortal Wkly Rep **56,** 4, 2007.
39. Roddy, E., Zhang, W., Doherty, M., Arden, N.K., Barlow, J., Birrell, F., *et al.* Evidence-based recommendations for the role of exercise in the management of osteoarthritis of the hip or knee—the MOVE consensus. Rheumatology (Oxford) **44,** 67, 2005.
40. Zhang, W., Doherty, M., Arden, N., Bannwarth, B., Bijlsma, J., Gunther, K.P., *et al.* EULAR evidence based recommendations for the management of hip osteoarthritis: report of a task force of the EULAR Standing Committee for International Clinical Studies Including Therapeutics (ESCISIT). Ann Rheum Dis **64,** 669, 2005.
41. Roberts, S., Menage, J., Sandell, L.J., Evans, E.H., and Richardson, J.B. Immunohistochemical study of collagen types I and II and procollagen IIA in human cartilage repair tissue following autologous chondrocyte implantation. Knee **16,** 398, 2009.
42. Zeifang, F., Oberle, D., Nierhoff, C., Richter, W., Moradi, B., and Schmitt, H. Autologous chondrocyte implantation using the original periosteum-cover technique versus matrix-associated autologous chondrocyte implantation: a randomized clinical trial. Am J Sports Med **38,** 924, 2010.
43. Chu, C.R., Szczodry, M., and Bruno, S. Animal models for cartilage regeneration and repair. Tissue Eng Part B Rev **16,** 105, 2010.
44. Kim, T.K., Sharma, B., Williams, C.G., Ruffner, M.A., Malik, A., McFarland, E.G., *et al.* Experimental model for cartilage tissue engineering to regenerate the zonal organization of articular cartilage. Osteoarthritis Cartilage **11,** 653, 2003.
45. Klein, T.J., Schumacher, B.L., Schmidt, T.A., Li, K.W., Voegtline, M.S., Masuda, K., *et al.* Tissue engineering of stratified articular cartilage from chondrocyte subpopulations. Osteoarthritis Cartilage **11,** 595, 2003.
46. Sharma, B., Williams, C.G., Kim, T.K., Sun, D., Malik, A., Khan, M., *et al.* Designing zonal organization into tissue-engineered cartilage. Tissue Eng **13,** 405, 2007.
47. Woodfield, T.B., Malda, J., de Wijn, J., Peters, F., Riesle, J., and van Blitterswijk, C.A. Design of porous scaffolds for cartilage tissue engineering using a three-dimensional fiber-deposition technique. Biomaterials **25,** 4149, 2004.
48. Farrell, E., Wielopolski, P., Pavljasevic, P., van Tiel, S., Jahr, H., Verhaar, J., *et al.* Effects of iron oxide incorporation for long term cell tracking on MSC differentiation *in vitro* and *in vivo*. Biochem Biophys Res Commun **369,** 1076, 2008.
49. Saldanha, K.J., Doan, R.P., Ainslie, K.M., Desai, T.A., and Majumdar, S. Micrometer-sized iron oxide particle labeling of mesenchymal stem cells for magnetic resonance imaging-based monitoring of cartilage tissue engineering. Magn Reson Imaging **29,** 40, 2011.
50. Yang, C.Y., Hsiao, J.K., Tai, M.F., Chen, S.T., Cheng, H.Y., Wang, J.L., *et al.* Direct labeling of hMSC with SPIO: the long-term influence on toxicity, chondrogenic differentiation capacity, and intracellular distribution. Mol Imaging Biol **13,** 443, 2011.
51. Kostura, L., Kraitchman, D.L., Mackay, A.M., Pittenger, M.F., and Bulte, J.W. Feridex labeling of mesenchymal stem cells inhibits chondrogenesis but not adipogenesis or osteogenesis. NMR Biomed **17,** 513, 2004.

Address correspondence to:
Darryl D. D'Lima, M.D., Ph.D.
Shiley Center for Orthopaedic Research and Education
Scripps Clinic
11025 North Torrey Pines Road
Suite 200
La Jolla, CA 92037

E-mail: dlima.darryl@scrippshealth.org

Received: September 17, 2011
Accepted: January 6, 2012
Online Publication Date: February 10, 2012